Genome-wide differential gene network analysis R software and its application in LnCap prostate cancer

Gökmen Altay[1*] and David E. Neal[2]

[1*]La Jolla Institute for Allergy and Immunology, CA, USA

[2]Nuffield Department of Surgical Sciences, University of Oxford, Headington, OX3 7DQ , Oxford, United Kingdom

*Corresponding author altay@lji.org

Abstract

We introduce an R software package for condition-specific gene regulatory network analysis based on DC3NET algorithm. We also present an application of it on a real prostate dataset and demonstrate the benefit of the software. We performed genome-wide differential gene network analysis with the software on the LnCap androgen stimulated and deprived prostate cancer gene expression datasets (GSE18684) and inferred the androgen stimulated prostate cancer specific differential network. As an outstanding result, CXCR7 along with CXCR4 appeared to have the most important role in the androgen stimulated prostate specific genome-wide differential network. This blind estimation is strongly supported from the literature. The critical roles for CXCR4, a receptor over-expressed in many cancers, and CXCR7 on mediating tumor metastasis, along with their contributions as biomarkers of tumor behavior as well as potential therapeutic target were studied in several other types of cancers. In fact, a pharmaceutical company had already developed a therapy by inhibiting CXCR4 to block non-cancerous immuno-suppressive and pro-angiogenic cells from populating the tumor for disrupting the cancer environment and restoring normal immune surveillance functions. Considering this strong confirmation, our inferred regulatory network might reveal the driving mechanism of LnCap androgen stimulated prostate cancer. Because, CXCR4 appeared to be in the center of the largest subnetwork of our inferred differential network. Moreover, enrichment analyses for the largest subnetwork of it appeared to be significantly enriched in terms of axon guidance, fc gamma R-mediated phagocytosis and endocytosis. This also conforms with the recent literature in the field of prostate cancer.

We demonstrate how to derive condition-specific gene targets from expression datasets on genome-wide level using differential gene network analysis. Our results showed that differential gene network analysis worked well in a prostate cancer dataset, which suggest the use of this approach as essential part of current expression data processing.

Availability: The introduced R software package available in CRAN at

https://cran.r-project.org/web/packages/dc3net and also at https://github.com/altayg/dc3net

Background

Prostate cancer is the second most common cancer in the male population, with an estimated 417,000 new cases diagnosed each year in Europe (Ferlay, 2013). The activation of androgen receptor (AR) through androgens plays a crucial role in the development and progression of prostate cancer (Kaur, 2016; Anantharaman, 2015; Choudhary, 2011; Massie, 2011). For early detection of prostate cancer, prostate specific antigen (PSA) screening method has been used widely as a diagnostic tool (Karatas, 2015). However, PSA fails to discriminate indolent disease which results in over-diagnosis and this may lead to poor prognosis (Abou-Ouf, 2015; Ma, 2015; Myers, 2015). Furthermore, there is no evidence showing that the PSA screening reduces the incidence of death and the underlying mechanism of prostate cancer progression remains largely unknown (Cannistraci, 2014 ;Ren, 2015).

Nowadays, the identification of novel oncogenes or tumor suppressor genes has become popular in tumorigenesis studies in understanding molecular mechanisms that drive disease progression (Ren, 2015). Understanding the working mechanism of molecules in normal cell physiology and pathogenesis allows subtle drug development and helps treatment of a disease, such as cancer (Altay, 2010; Rual, 2005; Schadt, 2009). The advent of systems and network biology enable us to capture interactions occurring within a cell, which can be represented as gene networks. Computational analysis of the networks provides key insights into biological pathways and cellular organization (Altay, 2011).

The biological processes at the gene level are very complex structures as genes dynamically interact with each other. The interactions of these molecules have been changing significantly over time and in different cell conditions such as from normal to cancer (Emmert-Streib, 2012; Califano, 2011). A single gene can participate in different biological processes and regulate different genes at different times. However, diseases are usually consequences of interactions between multiple molecular processes, rather than an abnormality in a single gene (Menche, 2015).

Gene regulatory networks hold the potential to identify specific subnetworks that are dysfunctional in the disease state of a cell. The identification of differences between disease and healthy tissues may provide key insights into the underlying mechanisms of diseases (de la Fuente, 2010; Ideker, 2012). For this purpose, several methods have been proposed in the literature. However, none of these methods, to our knowledge, provided direct physical interactions in the inferred differential network. Differential C3NET (DC3NET) algorithm was introduced to match that need (Altay, 2011), which is based on the very conservative gene regulatory network (GRN) inference algorithm C3NET (Altay, 2010). In order to ease the usage of DC3NET, we developed an R software, dc3net, and introduce it along with its application on a real dataset in this paper.

In the present study, differential gene network analysis has been performed to detect the differences between androgen stimulated and androgen deprived prostate cancer cells. We have used differential network inference software tool, dc3net, based on the algorithm DC3NET (Altay, 2011) and used it to infer androgen stimulated prostate cancer specific differential network which can be seen in Figure 1. We have performed validation study on our results via pathway analysis and with direct support from literature that substantiate our blind estimation on prostate cancer.

2. Materials and methods

2.1. Microarray data and data preprocessing

In order to investigate the alterations in androgen stimulated prostate cancer cells compared with androgen deprived prostate cancer cells, the microarray dataset, GSE18684 generated by Massie et al. (2011), was obtained from the Gene Expression Omnibus (GEO, http://www.ncbi.nlm.nih.gov/geo). The expression profile included 96 samples, comprising 20 androgen deprived tissue samples and 76 tissue samples with androgen stimulated prostate cancer. Sample size 76 is sufficient to infer gene network with maximum performance but sample size 20 may provide reduced performance according to (Altay, 2012).

The raw microarray data were analyzed using R software v.3.2.2 (http://www.r-project.org) and further processed using Affy package in Bioconductor (Gautier, 2004). The background correction, quantile normalization, and probe summarization processes were performed by the Robust Multi-array Average (RMA) algorithm to obtain gene expression matrix for each datasets (normal and tumor) (Irizarry, 2003).

In microarray technology, multiple probes can represent a single gene. In theory and mostly in practice those kinds of probes have highest association scores among them which cause an error for the inference algorithm *c3net* as it infers only the highest correlated pair for each significant gene. When one works at the probe level data, one should address this issue. In order to eliminate this problem, we filter the association matrix by setting zero for the mutual information score for those probe pairs that correspond to the same gene (Altay, 2010). We have developed a function in the package to practically ease to overcome this issue.

2.2. Differential network analysis

In order to perform genome-wide differential gene network analysis, we used the software tool dc3net which is available in CRAN (https://cran.r-project.org/web/packages/dc3net). Briefly, the dc3net algorithm takes two different microarray gene expression data sets as input (e.g. one as tumor and the other as control). Then, two different gene networks are inferred by applying C3NET (Altay, 2010, Altay, 2010) to each of the data sets. In order to compute dependency scores among genes, we used PBG that computes mutual information values that provide sufficient performance with very low complexity (Kurt, 2014).

In the final step, these two networks are compared and tumor differential network and common network are inferred. The tumor differential network, *difnet*, is inferred by selecting only the interactions of tumor differential network that does not strong association scores in the control network. The common network, *comnet*, is determined by selecting the overlapping or closer interactions in value or rank between the two networks (Altay, 2011).

In this study, we used the differential network inference all-in-one function *dc3net* with those parameters as follows, where the further details can be seen in the CRAN repository:

"*dc3net(test_data, control_data, probe_names, gene_names, method="cutoff", methodValue=0, itNum=1, rankDif=2000, percentDif=0.3, rankdCom=100, percentCom=0.6, probFiltered=FALSE, visualization=TRUE)"*

2.3. Gene ontology analysis

Gene Ontology (GO) enrichment analysis based on Gene Ontology database (http://www.geneontology.org) was performed to investigate the biological roles of the genes in the differential network (da Huang, 2009). To further assess the signalling pathway of the

genes, we subsequently performed Kyoto Encyclopedia of Genes and Genomes (KEGG, http://www.genome.jp/kegg) pathway enrichment analysis. The two analysis were performed using The Database for Annotation, Visualization and Integrated Discovery (DAVID, https://david.ncifcrf.gov) which is a powerful bioinformatics tool to find out functions of interested genes (Dennis, 2003). The enrichment analyses required >5 genes to be present and $p<0.05$ for a term to be considered significant.

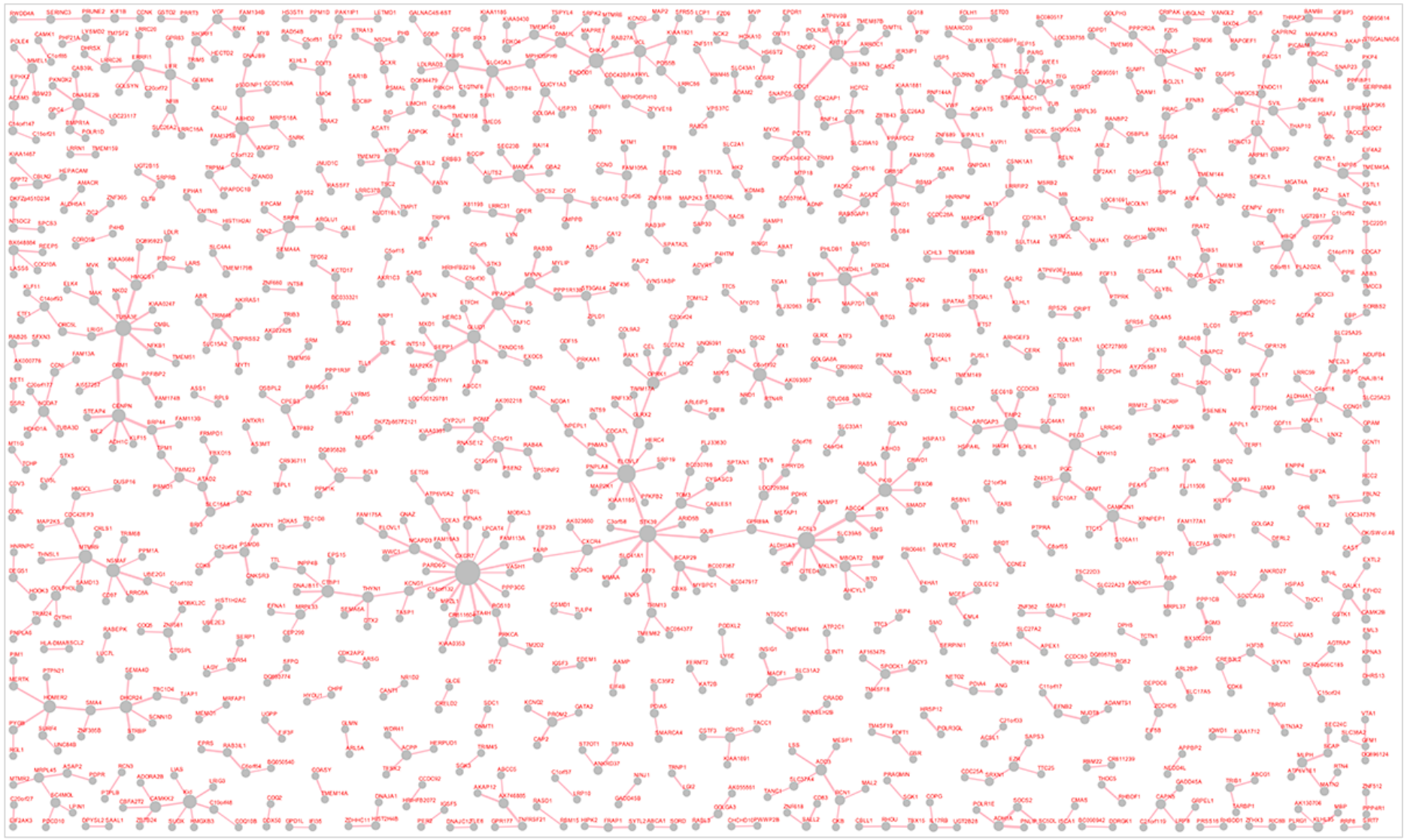

Figure 1. Genome-wide androgen stimulated prostate specific differential network with 891 interactions

3. Results

3.1. Inferring differential network

The androgen stimulated prostate cancer differential gene network with 891 interactions was inferred using the dc3net tool where details of its usage can be seen in the Supplementary File. The largest independent subnetwork with 119 interactions were also extracted from the differential network and plotted as in Figure 3.

3.2. Functional enrichment analysis

To investigate the functions of the genes in the androgen stimulated prostate cancer differential gene network, GO and KEGG pathway analysis were performed. A total 184 terms were retrieved from the DAVID online analytical tool.

The top ten GO terms ranked by statistical significance were listed in Table 1. GO analysis revealed that genes associated with sterol biosynthetic process (GO:0016126; p=5.05 e-08), protein transport (GO:0015031; p=2.57 e-07) and establishment of protein localization (GO:0045184; p=3.80 e-07) were significantly enriched top three GO terms among biological processes, while for molecular functions, nucleotide binding (GO:0000166; p=7.08 e-05), purine nucleotide binding (GO:0017076; p=5.22 e-04) and purine ribonucleotide binding (GO:0032555; p=9.11 e-04) were significantly enriched, and with regards to cellular components, genes associated with endoplasmic reticulum (GO:0005783; p=2.66 e-13), endoplasmic reticulum part (GO:0044432; p=1.16 e-06) and organelle membrane (GO:0031090; p=1.48 e-04) were significantly enriched (Table 1, Fig. 2A).

Table 1. GO terms of differential network (top 10).

GO ID	GO term	No. of genes	p
Biological processes			
GO:0016126	sterol biosynthetic process	14	5.05E-08
GO:0015031	protein transport	82	2.57E-07
GO:0045184	establishment of protein localization	82	3.80E-07
GO:0046907	intracellular transport	73	3.96E-07
GO:0006695	cholesterol biosynthetic process	11	1.25E-06
GO:0016125	sterol metabolic process	21	1.87E-06
GO:0006886	intracellular protein transport	47	2.61E-06
GO:0008104	protein localization	87	4.16E-06
GO:0034613	cellular protein localization	49	6.76E-06
GO:0008203	cholesterol metabolic process	19	7.26E-06
Cellular components			
GO:0005783	endoplasmic reticulum	117	2.66E-13
GO:0044432	endoplasmic reticulum part	46	1.16E-06
GO:0031090	organelle membrane	97	1.48E-04
GO:0005789	endoplasmic reticulum membrane	33	2.11E-04
GO:0042175	nuclear envelope-endoplasmic reticulum network	34	2.63E-04
GO:0005739	mitochondrion	92	9.73E-04
GO:0005829	cytosol	109	9.89E-04
GO:0005792	microsome	28	1.24E-03
GO:0005624	membrane fraction	71	1.61E-03
GO:0042598	vesicular fraction	28	1.90E-03
Molecular Function			
GO:0000166	nucleotide binding	174	7.08E-05
GO:0017076	purine nucleotide binding	147	5.22E-04
GO:0032555	purine ribonucleotide binding	140	9.11E-04
GO:0032553	ribonucleotide binding	140	9.11E-04
GO:0000287	magnesium ion binding	42	4.10E-03
GO:0001883	purine nucleoside binding	119	5.75E-03
GO:0003924	GTPase activity	23	6.81E-03
GO:0001882	nucleoside binding	119	7.19E-03
GO:0005524	ATP binding	110	7.74E-03
GO:0004674	protein serine/threonine kinase activity	39	8.48E-03

FDR: false discovery rate; GO: gene ontology.

Next, the genes found in the androgen stimulated prostate cancer differential gene network were submitted to DAVID server to identify significantly enriched KEGG pathways (Kanehisa, 2000; Kanehisa, 2012). The KEGG pathways that were found significantly enriched ($p<0.05$) are shown in Table 2. Pathway analysis revealed that the genes in the androgen stimulated prostate cancer difnet were significantly enriched in ten terms. The most significant three terms were those involved in steroid biosynthesis (p=2.80 e-07), synthesis and degradation of ketone bodies (p=1.646523 e-03), and amino sugar and nucleotide sugar metabolism (p=1.73 e-03) processes (Fig. 2B).

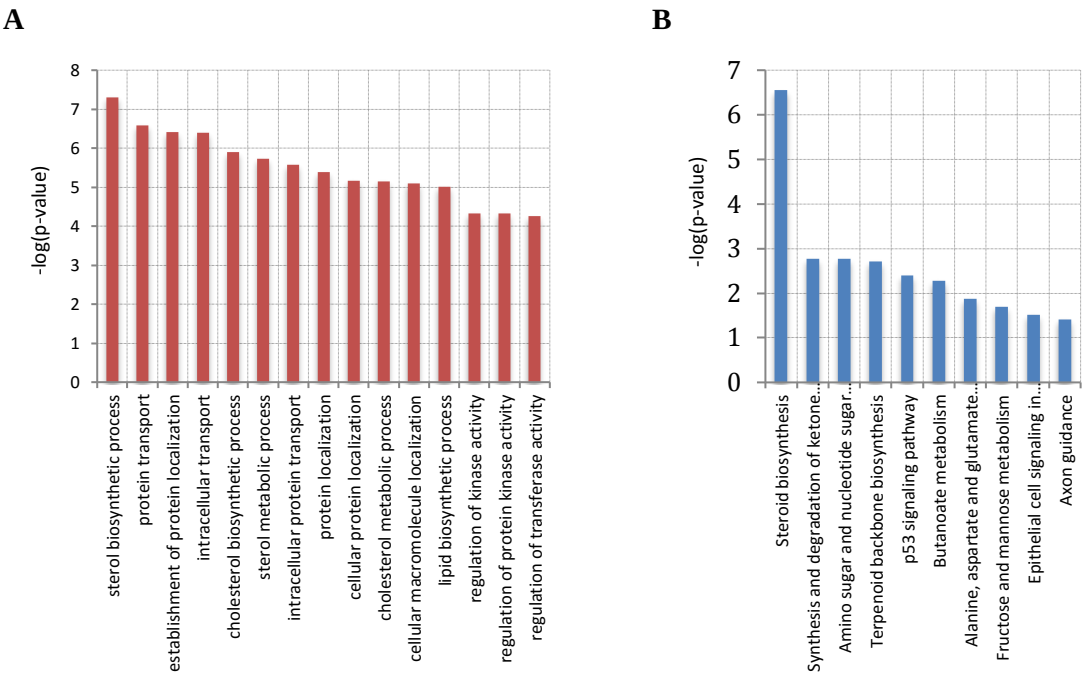

Figure 2. Functional annotation of significantly enriched genes in differential network. (A) The top 10 enriched gene ontology categories for biological processes; (B) The enriched Kyoto Encyclopedia of Genes and Genomes pathways.

Table 2. Significant KEGG pathways in the androgen stimulated prostate cancer specific differential network

KEGG ID	KEGG term	No. of genes	p	Genes
hsa00100	Steroid biosynthesis	10	2.80E-07	TM7SF2, CEL, EBP, SQLE, LSS, SC5DL, DHCR24, FDFT1, SC4MOL, NSDHL
hsa00072	Synthesis and degradation of ketone bodies	5	1.69E-03	HMGCS2, HMGCS1, ACAT2, ACAT1, HMGCL
hsa00520	Amino sugar and nucleotide sugar metabolism	10	1.71E-03	PGM2, GMPPB, GALK1, PGM3, GNPDA1, CMAS, GFPT1, GFPT2, HK2, GALE
hsa00900	Terpenoid backbone biosynthesis	6	1.95E-03	HMGCS2, HMGCS1, FDPS, MVK, ACAT2, ACAT1
hsa04115	p53 signaling pathway	12	3.94E-03	CCNE2, BID, PPM1D, TSC2, SIAH1, CDK6, CCNG1, GADD45B, THBS1, IGFBP3, GADD45A, SESN3
hsa00650	Butanoate metabolism	8	5.33E-03	ACSM3, HMGCS2, ALDH5A1, HMGCS1, ABAT, ACAT2, ACAT1, HMGCL
hsa00250	Alanine, aspartate and glutamate metabolism	7	1.32E-02	ASS1, ALDH5A1, GFPT1, GLUD1, GFPT2, ABAT, ALDH4A1
hsa00051	Fructose and mannose metabolism	7	2.05E-02	MTMR2, GMPPB, SORD, PFKFB2, HK2, PFKM, MTMR6
hsa05120	Epithelial cell signaling in Helicobacter pylori infection	10	3.03E-02	IGSF5, ATP6V0E1, LYN, ATP6V1E1, MAP2K4, NFKB1, PAK1, JAM3, ATP6V0A2, ATP6V0B
hsa04360	Axon guidance	15	3.89E-02	NRP1, EFNB3, EFNA1, EFNB2, DPYSL2, EPHA1, SEMA6A, NCK2, PAK2, CXCR4, PPP3CC, EFNA5, PAK1, SEMA4D, SEMA4A

KEGG: Kyoto Encylopedia of genes and genomes

In order to further evaluate the biological roles of the genes in the independent subnetworks of the genome wide androgen stimulated prostate cancer difnet, we performed KEGG analysis for the largest subnetwork. As shown on Figure 3, this subnetwork comprises 119 interactions with CXCR7, STK39, ELOVL3 and ACSL3 at the center of the largest hubs. KEGG analysis of the genes included in the subnetwork revealed a highly significant association with axon guidance pathway (p=1.71 e-03), which was also found significantly enriched in the whole differential network. Furthermore, pathways involved in Fc gamma R-mediated phagocytosis (p=2.69 e-02) and Endocytosis (p=3.62 e-02) were also highly enriched (Table 3). Interestingly, these two pathways were not found significantly enriched in the whole differential network.

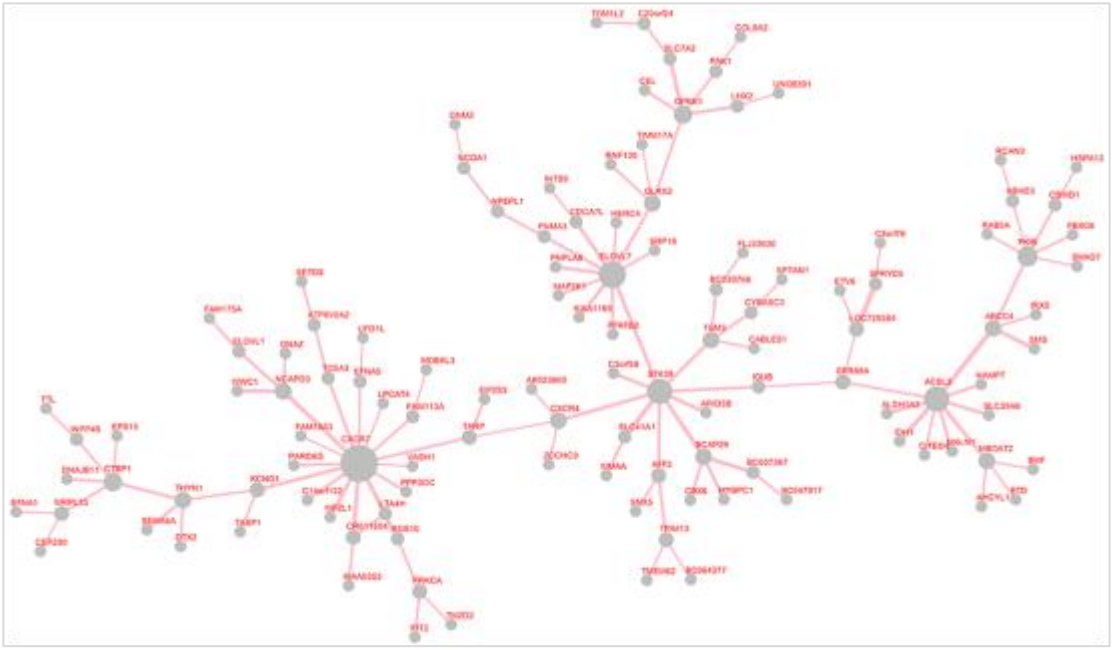

Figure 3. The largest connected subnetwork of the androgen stimulated prostate cancer difnet. This subnetwork might have an important role in human prostate cancer as being the largest connected subnetwork with 119 edges in tumor difnet.

Table 3. Significant KEGG pathways in the largest subnetwork of the androgen stimulated prostate cancer specific differential network

KEGG ID	KEGG term	No. of genes	p	Genes
hsa04360	Axon guidance	6	1.71E-03	SEMA6A, CXCR4, EFNA1, PPP3CC, EFNA5, PAK1
hsa04666	Fc gamma R-mediated phagocytosis	4	2.69E-02	PRKCA, MAP2K1, PAK1, DNM2
hsa04144	Endocytosis	5	3.62E-02	EPS15, CXCR4, RAB5A, PARD6G, DNM2

KEGG: Kyoto Encylopedia of genes and genomes

4. Discussion

By employing differential gene network analysis approach, the present study aims to investigate the molecular mechanisms that may drive disease progression in prostate cancer using our presented software dc3net.

Top four hub nodes, identified in the present study, have been strongly associated with prostate cancer metastatic process, including CXCR7, STK39, ELOVL7 and ACSL3. Hub nodes are genes that are highly connected with other genes and they were proposed to have important roles in biological development. Since hub nodes have more complex interactions than other genes, they may have crucial roles in the underlying mechanisms of disease (Guo, 2015). Identification of hub genes involved in progression of prostate cancer may lead to the development of better diagnostic methods and providing therapeutic approaches.

According to our analysis, CXCR7 (chemokine (C-X-C motif) receptor 7) is by far the top hub gene in the androgen stimulated differential network and it is also part of the largest independent subnetwork as seen in Figure 3. In (Wang, 2008), it is reported that staining of high-density tissue microarrays shows that the levels of CXCR7/RDC1 expression increase as the tumors become more aggressive. Also, *In vitro* and *in vivo* studies with prostate cancer cell lines propose that alterations in CXCR7/RDC1 expressions are associated with enhanced invasive and adhesive activities in addition to a survival advantage. Along other papers on CXCR7 (Zheng, 2010), it was shown that increased CXCR7 expression was found in hepatocellular carcinoma (HCC) tissues. Knockdown of CXCR7 expression by transfected with CXCR7shRNA significantly inhibited SMMC-7721 angiogenesis, adhesion and cells invasion. Moreover, down-regulation of CXCR7 expression leads to a reduction of tumor growth in a xenograft model of HCC (Zheng, 2010). Another study demonstrated that the IL-8–regulated Chemokine Receptor CXCR7 stimulates EGFR Signaling to promote prostate cancer growth (Singh, 2011). In a study conducted by Yun *et al.*, it is reported that CXCR7 expression is increased in most of the tumor cells compared with the normal cells and is involved in cell proliferation, migration, survival, invasion and angiogenesis during the initiation and progression of many cancer types including prostate cancer (Yun, 2015). A more recent study indicated that there appeared to be disconnect of the effect of DHT on CXCL12/CXCR4/CXCR7 chemokine axis between transcriptional and translation machinery in androgen-responsive LnCaP cell line. There are many other studies that showed the strong role of CXCR7 in metastatic type cancer that strongly validates our blind foremost prediction is very likely to be true and thus needs further experimental work on its targets that we inferred in this study. However,

It was also observed that CXCR7/RDC1 levels are regulated by CXCR4 (Singh, 2011). This is a very interesting supporting information from literature for our blind estimation because in our predicted largest independent subnetwork, as shown in Figure 3, CXCR7 and CXCR4 appear to be very close and interacting over only one gene. Although CRCX4 is not a hub gene, it appears to be as a bridge that connects both halves of the largest subnetwork. According to KEGG analysis, CXCR4 was found in the gene list of two different significantly enriched KEGG pathways, axon guidance and endocytosis which are strongly associated with prostate cancer (Table 3). Considering the prediction was made on global level, this literature confirmation seems assuring but not a coincidence. Therefore, this relation is worth experimenting in LnCap cancer too. It is also reported (Shanmugam, 2011) that inhibition of CXCR4/CXCL12 signaling axis by ursolic acid leads to suppression of metastasis in transgenic adenocarcinoma of mouse prostate model and CXCR4 induced a more aggressive phenotype in prostate cancer (Miki, 2007). In another study, it is reported that CXCR4 and CXCR7 have critical roles on mediating tumor metastasis in various types of cancers as both being a receptor for an important α-chemokine, CXCL12 (Sun, 2010). Furthermore, a more recent study concluded that CXCR4 plays a crucial role in cancer proliferation, dissemination and invasion and the inhibition of CXCR4 strongly affects prostate cancer metastatic disease (Gravina, 2015). The chief officer of Massachusetts based X4 Pharmaceuticals company recently stated that CXCR4 protein "acts as a beacon to attract cells to surround a tumor, effectively hiding the tumor from the body's T cells that would otherwise destroy them". He indicated that X4 company is beginning human trials using CXCR4 inhibitors which aims to develop a therapy to block the protein, CXCR4 (http://pharmaceuticalintelligence.com/2015/12/15/are-cxc4-antagonists-making-a-comeback-in-cancer-chemotherapy, 2015).

The second most likely prediction was STK39 (serine threonine kinase 39). Among others, in (Hendriksen, 2006) it is reported that lower mRNA expression of STK39 in primary prostate tumors was correlated with a higher incidence of metastases after radical prostatectomy. In (Balatoni, 2009), it is stated that STK39 encoded protein SPAK, regulates cell stress responses, and microarray studies identified reduced SPAK expression in treatment-resistant breast cancers and metastatic prostate cancers, suggesting that its loss may play a role in cancer progression. They showed that epigenetic silencing of STK39 in B-cell lymphoma inhibits apoptosis from genotoxic stress in cancer. STK39 is also identified as hypertension susceptibility gene (Wang, 2008).

ELOVL7 (fatty acid elongase 7) was reported that it could be involved in prostate cancer cell growth and survival through the metabolism of SVLFAs and their derivatives, could be a key molecule to elucidate the association between fat dietary intake and prostate carcinogenesis, and could also be a promising molecular target for development of new therapeutic or preventive strategies for prostate cancers (Tamura, 2009).

ACSL3 (acyl-CoA synthetase long-chain family member 3) was reported to be one of the androgen-regulated genes and it is shown that ACSL3 is slightly up-regulated in primary prostate tumors and strongly repressed in metastatic cancer (Marques, 2011). It also states that ACSL3, ELOVL5 and GLUD1 play a role in the production of prostatic fluid and in secretory function of the prostate. From this literature information, it worth mentioning that we blindly predicted ACSL3, ELOVL7 and GLUD1 as in top eight tumor-specific hubs, which may suggest their collaborative role in this disease from this biological process. There is also a patent that reports that the fusion genes ACSL3 and ETV1 and their expression

products can be used as prognostic and diagnostic markers for prostate cancer and as clinical targets for the treatment of prostate cancer (Attard, 2008).

In order to investigate biological functions of the genes in the differential network, GO and KEGG pathway enrichment analyses were performed. The pathway analysis is important since it improves disease classification and reveals novel insights about a disease (Myers, 2015). The results showed that sterol biosynthetic process was the most significantly enriched GO term for biological process. To further evaluate the biological roles of the genes in the differential network, KEGG pathway analysis was performed. According to the KEGG analysis, Steroid biosynthesis was the most significant pathway (p=2.80 e-07). It contains ten genes in our network: TM7SF2, CEL, EBP, SQLE, LSS, SC5DL, DHCR24, FDFT1, SC4MOL and NSDHL. The relation of Steroid biosynthesis and prostate cancer is reported in many studies. The ligand activation of the androgen receptor plays an important role in the progress of castration-resistant prostate cancers. The similarities and differences from glandular androgen synthesis provide direction for the development of new treatments (Migita, 2009; Sharifi, 2012; Auchus, 2012; Ferraldeschi, 2013).

The pathway with the second highest significance was the synthesis and degradation of ketone bodies pathway (p=1.63 e-03), which contains five genes: HMGCS2, HMGCS1, ACAT2, ACAT1 and HMGCL. In the study conducted by Lin et. al. (2005), synthesis and degradation of ketone bodies pathway found as up-regulated pathway in androgen-independent CL1 cells (model for late-stage prostate cancer) when compared to androgen-dependent LnCaP (model for early-stage prostate cancer) cells.

We have also examined the other significant pathways, and found that Amino sugar and nucleotide sugar metabolism (Priolo, 2014), p53 signaling pathway (Chappell, 2012; Gupta, 2012; Stegh, 2012), Butanoate metabolism (Stoss, 2008; Romanuik, 2010), Alanine, aspartate and glutamate metabolism (Priolo, 2014), and Axon guidance (Choi, 2014) pathways were shown to be associated with the prognosis of prostate cancer. In these pathways, the p53 signaling pathway plays a critical role in cancer's response to chemotherapy and tumor growth. Inactivation of the tumor suppressor gene p53 is widely observed in more than 50% of human cancers including prostate cancer. The disruption of the p53 signaling pathway is one of the vital turning point for the survival of advanced prostate cancer cells during therapies. By enabling DNA repair, it was observed that p53 blocks cancer progression by provoking transient or permanent growth arrest (Chappell, 2012; Gupta, 2012; Stegh, 2012). However, three pathways, Terpenoid backbone biosynthesis (hsa00900), Fructose and mannose metabolism (hsa00051) and Epithelial cell signaling in Helicobacter pylori infection (hsa05120), have not previously been related to prostate cancer.

KEGG analysis for the largest independent subnetwork revealed much more interesting results that may show that it has the most important role in the prostate cancer. Axon guidance (hsa04360) pathway, which was also found significantly enriched in the whole differential network, is known to have tumor suppressor genes and therefore related with tumor growth. Axon guidance molecules are validated as tumor suppressor in the breast cancer and show promise as breast cancer diagnostic markers as well as potential therapeutic targets (Mehlen, 2011; Harburg, 2011). In the study conducted by Choi, axon guidance pathway was shown to be involved in prostate cancer tumorigenesis (Choi, 2014). In addition, Savli et al. reported that axon guidance signaling pathway was the most significant down-regulated canonical pathway in prostate cancer (Savli, 2008). The second significantly enriched pathway was Fc gamma R-mediated phagocytosis (hsa04666). This pathway was

found as the highest significant pathway in prostate cancer and have been referred as being involved in the pathological development of prostate cancer (Jia, 2012). In the literature, the pathway endocytosis (hsa04144), was also found related with prostate cancer. The importance of understanding the regulation between signal transduction and endocytosis pathways, and also how the breakdown of this integrated regulation contributes to cancer development was emphasized (Bonaccorsi, 2007).

In briefly, our top four strongest blind predictions were all validated in the literature. One can now experiment these top 4 hubs in LnCap cell lines to elucidate the role of them in prostate cancer considering our predicted targets of them. Additionally, KEGG pathway analysis on our androgen stimulated prostate cancer specific differential network has revealed outstanding results. According to the KEGG pathway analysis results, out of ten most significantly enriched pathways, seven of them are already known to have a strong association with prostate cancer. We have made our disease specific network inference with a blind prediction and it is mostly validated by the pathway analysis. We suggest that the three unrelated pathways with prostate cancer are promising candidate pathways that need to be experimentally investigated in order to reveal the relation of them with prostate. More interestingly, KEGG pathway analysis in the largest independent subnetwork of our androgen stimulated prostate cancer difnet, has revealed three pathways where all of them known to have strong association with prostate cancer. This shows the highly accurate performance of the differential network analysis tool dc3net. We considered that this largest subnetwork as the most important mechanism for prostate cancer in our androgen stimulated prostate cancer difnet.

5. Conclusions

The present study provided significant insight into the molecular mechanisms associated with prostate cancer. Furthermore, GO and KEGG pathway enrichment analysis identified numerous pathways that may have a role in the prostate cancer, and these findings may promote the better understanding about the molecular mechanism of this disease and also disclose potential targets for diagnostic and effective therapies. Some of our estimations in the androgen stimulated prostate cancer difnet may well be biomarkers or drug targets for prostate cancer and awaits biologist to perform wet-lab experiments on them.

Acknowledgement

There is one more contributor to this manuscript but he left the study at the final stage with no notification at all. He had contributed sufficiently to be a co-author but did not respond our several contact attempts and did not provide his affiliation to be included in the manuscript.

References

Abou-Ouf H, Zhao L, Bismar TA. ERG expression in prostate cancer: biological relevance and clinical implication. J Cancer Res Clin Oncol. 2015.

Altay G. Empirically determining the sample size for large-scale gene network inference algorithms. IET Syst. Biol. 2012;6:35-63.

Altay G, Asim M, Markowetz F, Neal DE. Differential C3NET reveals disease networks of direct physical interactions. BMC Bioinformatics; 2011;12:296.

Altay G, Emmert-Streib F. Inferring the conservative causal core of gene regulatory networks. BMC Syst. Biol. 2010;4:132.

Altay G, Emmert-Streib F. Revealing differences in gene network inference algorithms on the network level by ensemble methods. Bioinformatics. 2010;26(14):1738-44.

Anantharaman A, Friedlander TW. Targeting the androgen receptor in metastatic castrate-resistant prostate cancer: A review. Urol Oncol. 2015;S1078-1439(15)00555-4.

Attard G, Clark J, Ambroisine L, Mills IG, Fisher G. et al. Heterogeneity and clinical significance of ETV1 translocations in human prostate cancer. Br J Cancer. 2008;99(2):314-20.

Auchus ML, Auchus RJ. Human steroid biosynthesis for the oncologist. J Investig Med. 2012 Feb;60(2):495-503.

Balatoni CE, Dawson DW, Suh J, Sherman MH, Sanders G, Hong JS, Frank MJ, Malone CS, Said JW, Teitell MA. Epigenetic silencing of Stk39 in B-cell lymphoma inhibits apoptosis from genotoxic stress. Am J Pathol. 2009;175(4):1653-61

Bonaccorsi L, Nosi D, Muratori M, Formigli L, Forti G, Baldi E. Altered endocytosis of epidermal growth factor receptor in androgen receptor positive prostate cancer cell lines. J Mol Endocrinol. 2007;38(1-2):51-66.

da Huang W, Sherman BT, Lempicki RA. Bioinformatics enrichment tools: paths toward the comprehensive functional analysis of large gene lists. Nucleic Acids Res. 2009;37:1-13.

Califano R, Griffiths R, Lorigan P, Ashcroft L, Taylor P et al. Randomised phase II trial of 4 dose levels of single agent docetaxel in performance status (PS) 2 patients with advanced non-small cell lung cancer (NSCLC): DOC PS2 trial. Manchester lung cancer group. Lung Cancer. 2011 Sep;73(3):338-44.

Cannistraci A, Di Pace AL, De Maria R, Bonci D. MicroRNA as new tools for prostate cancer risk assessment and therapeutic intervention: Results from clinical data set and patients' samples. Biomed Res Int 2014;2014:146170.

Castro MAA. et al. RedeR: R/Bioconductor package for representing modular structures, nested networks and multiple levels of hierarchical associa-tions. Genome Biology; 2012:13(4):R29.

Chappell WH, Lehmann BD, Terrian DM, Abrams SL, Steelman LS, McCubrey JA. p53 expression controls prostate cancer sensitivity to chemotherapy and the MDM2 inhibitor Nutlin-3. Cell Cycle. 2012;11(24):4579-4588.

Choi, YJ, Yoo NJ, Lee SH. Down-regulation of ROBO2 Expression in Prostate Cancers. Pathol Oncol Res. 2014;20(3):517-519.

Choudhary V, Kaddour-Djebbar I, Lakshmikanthan V, Ghazaly T, Thangjam GS, Sreekumar A, Lewis RW, Mills IG, Bollag WB, Kumar MV. Novel role of androgens in mitochondrial fission and apoptosis. Mol Cancer Res. 2011;9(8):1067-77.

de la Fuente A. From 'differential expression' to 'differential networking' - identification of dysfunctional regulatory networks in diseases. Trends Genet; 2010:26(7):326-333.

Dennis G Jr, Sherman BT, Hosack DA, Yang J, Gao W, Lane HC, Lempicki RA. DAVID: database for annotation, visualization, and integrated discovery. Genome Biol. 2003;4:3.

Emmert-Streib F, Tripathi S, Simoes RM. Harnessing the complexity of gene expression data from cancer: from single gene to structural pathway methods. Biology Direct. 2012;7:44.

Ferlay J, Steliarova-Foucher E, Lortet-Tieulent J, Rosso S, Coebergh JW, Comber H, Forman D, Bray F. Cancer incidence and mortality patterns in Europe: estimates for 40 countries in 2012. Eur J Cancer. 2013;49(6):1374-403.

Ferraldeschi R, Sharifi N, Auchus RJ, Attard G. Molecular Pathways: Inhibiting steroid biosynthesis in prostate cancer. Clin Cancer Res. 2013;19(13):3353-3359.

Gautier L, Cope L, Bolstad BM, Irizarry RA. affy - analysis of Affymetrix GeneChip data at the probe level. Bioinformatics. 2004;20(3):307-315.

Gravina GL, Mancini A, Muzi P, Ventura L, Biordi L, Ricevuto E, Pompili S, Mattei C, Di Cesare E, Jannini EA, Festuccia C. CXCR4 pharmacogical inhibition reduces bone and soft tissue metastatic burden by affecting tumor growth and tumorigenic potential in prostate cancer preclinical models. Prostate. 2015 Sep;75(12):1227-46.

Guo X, Wang Y, Wang C, Chen J. Identification of several hub-genes associated with periodontitis using integrated microarray analysis. Mol Med Rep. 2015;11(4):2541-7.

Gupta K, Thakur VS, Bhaskaran N, Nawab A, Babcook MA, Jackson MW, Gupta S. Green tea polyphenols induce p53-dependent and p53-independent apoptosis in prostate cancer cells through two distinct mechanisms. PLoS One. 2012;7(12):e52572.

Harburg GC, Hinck L. Navigating Breast Cancer: Axon Guidance Molecules as Breast Cancer Tumor Suppressors and Oncogenes. J Mammary Gland Biol Neoplasia. 2011;16(3):257-270.

Hendriksen PJ, Dits NF, Kokame K, Veldhoven A, van Weerden WM, Bangma CH, Trapman J, Jenster G. Evolution of the androgen receptor pathway during progression of prostate cancer. Cancer Res. 2006;66(10):5012-20.

Ideker T, Krogan NJ. Differential network biology. Molecular Systems Biology. 2012;8:565.

Irizarry RA, Hobbs B, Collin F, et al. Exploration, normalization, and summaries of high density oligonucleotide array probe level data. Biostatistics. 2003;4(2):249-264.

Jia P, Liu Y, Zhao Z. Integrative pathway analysis of genome-wide association studies and gene expression data in prostate cancer. BMC Systems Biology. 2012;6(3):13.

Kanehisa M, Goto, S. KEGG: Kyoto Encyclopedia of Genes and Genomes. Nucleic Acids Research. 2000;28(1):27-30.

Kanehisa M, Goto S, Sato Y, Furumichi M, Tanabe M. KEGG for integration and interpretation of large-scale molecular data sets. Nucleic Acids Res. 2012;40:109-114.

Karatas OF, Guzel E, Duz MB, Ittmann M, Ozen M. The role of ATP-binding cassette transporter genes in the progression of prostate cancer. Prostate. 2015 Dec 28. doi: 10.1002/pros.23137. [Epub ahead of print].

Kaur P, Khatik GL. Advancements in Non-steroidal Antiandrogens as Potential Therapeutic Agents for the Treatment of Prostate Cancer. Mini Rev Med Chem. 2016. [Epub ahead of print]

Kurt Z, Aydin N, Altay G. A comprehensive comparison of association estimators for gene network inference algorithms. Bioinformatics. 2014;30(15): 2142-2149.

Li X, Li T, Chen D, Zhang P, Song Y, Zhu H, Xiao Y, Xing Y. Overexpression of lysine-specific demethylase 1 promotes androgen-independent transition of human prostate cancer LNCaP cells through activation of the AR signaling pathway and suppression of the p53 signaling pathway. Oncol Rep. 2016;35(1):584-92.

Lin B, White JT, Lu W, Xie T, Utleg AG, Yan X, Yi EC, Shannon P, Khrebtukova I, Lange PH, Goodlett DR, Zhou D, Vasicek TJ, Hood L. Evidence for the Presence of Disease-Perturbed Networks in Prostate Cancer Cells by Genomic and Proteomic Analyses: A Systems Approach to Disease. Cancer Res. 2005;65(8):3081-91.

Ma H, Schadt EE, Kaplan LM, Zhao H. COSINE: COndition-SpecIfic sub-NEtwork identification using a global optimization method. Bioinformatics. 2011;27(9):1290-8.

Ma D, Zhou Z, Yang B, He Q, Zhang Q, Zhang X. Association of molecular biomarkers expression with biochemical recurrence in prostate cancer through tissue microarray immunostaining. Oncol Lett. 2015; 10(4): 2185–2191.

Marques RB, Dits NF, Erkens-Schulze S, van Ijcken WF, van Weerden WM, Jenster G. Modulation of androgen receptor signaling in hormonal therapy-resistant prostate cancer cell lines. PLoS One. 2011;6(8):e23144.

Massie CE, Lynch A, Ramos-Montoya A, Boren J et al. The androgen receptor fuels prostate cancer by regulating central metabolism and biosynthesis. EMBO J. 2011;30(13):2719-33.

Mehlen P, Delloye-Bourgeois C, Chédotal A. Novel roles for Slits and netrins: axon guidance cues as anticancer targets? Nature Reviews Cancer. 2011;11:188-197.

Menche J, Sharma A, Kitsak M, Ghiassian S, Vidal M, et al. Uncovering disease-disease relationships through the incomplete human interactome. Science. 2015:347:6224.

Migita T, Ruiz S, Fornari A, Fiorentino M, Priolo C, Zadra G, Inazuka F, Grisanzio C, Palescandolo E, Shin E, Fiore C, Xie W, Kung AL, Febbo PG, Subramanian A, Mucci L, Ma J, Signoretti S, Stampfer M, Hahn WC et al. Fatty acid synthase: a metabolic enzyme and candidate oncogene in prostate cancer. J Natl Cancer Inst. 2009;101:519-532

Miki J, Furusato B, Li H, Gu Y, Takahashi H, Egawa S, Sesterhenn IA, McLeod DG, Srivastava S, Rhim JS. Identification of putative stem cell markers, CD133 and CXCR4, in hTERT-immortalized primary nonmalignant and malignant tumor-derived human prostate epithelial cell lines and in prostate cancer specimens. Cancer Res. 2007;67(7):3153-61.

Mirzayans R, Andrais B, Scott A, Murray D. New Insights into p53 Signaling and Cancer Cell Response to DNA Damage: Implications for Cancer Therapy. Journal of Biomedicine & Biotechnology. 2012;2012:1.

Myers JS, Lersner AK, Robbins CJ, Sang QA. Differentially Expressed Genes and Signature Pathways of Human Prostate Cancer. PLoS One. 2015; 10(12): e0145322.

Romanuik TL, Wang G, Morozova O, Delaney A, Marra MA, Sadar MD. LNCaP Atlas: Gene expression associated with in vivo progression to castration-recurrent prostate cancer. BMC Medical Genomics. 2010;3:43.

Priolo C, Pyne S, Rose J, Regan ER, Zadra G, Photopoulos C, Cacciatore S, Schultz D, Scaglia N, McDunn J, De Marzo AM, Loda M. AKT1 and MYC induce distinctive metabolic fingerprints in human prostate cancer. Cancer Res. 2014;74(24):7198-204.

Ren W, Li C, Duan W, Du S, Yang F, Zhou J, Xing J. MicroRNA-613 represses prostate cancer cell proliferation and invasion through targeting Frizzled7. Biochemical and Biophysical Research Communications. 2015. doi: 10.1016/j.bbrc.2015.12.054. [Epub ahead of print].

Rual JF, Venkatesan K, Hao T, Hirozane-Kishikawa T, Dricot A et al. Towards a proteome-scale map of the human protein-protein interaction network. Nature. 2005;437(7062):1173-8.

Savli H, Szendröi A, Romics I, Nagy B. Gene network and canonical pathway analysis in prostate cancer: a microarray study. Exp Mol Med. 2008;40(2):176-185.

Schadt EE. Molecular networks as sensors and drivers of common human diseases. Nature. 2009;461(7261):218-23.

Shanmugam MK, Rajendran P, Li F, Nema T, Vali S, Abbasi T, Kapoor S, Sharma A, Kumar AP, Ho PC, Hui KM, Sethi G. Ursolic acid inhibits multiple cell survival pathways leading to suppression of growth of prostate cancer xenograft in nude mice. J Mol Med (Berl). 2011;89(7):713-27.

Sharifi N, Auchus RJ. Steroid biosynthesis and prostate cancer. Steroids. 2012;77(7):719-726.

Singh RK1, Lokeshwar BL. The IL-8-regulated chemokine receptor CXCR7 stimulates EGFR signaling to promote prostate cancer growth. Cancer Res. 2011;71(9):3268-77.

Stegh, AH. Targeting the p53 signaling pathway in cancer therapy - The promises, challenges, and perils. Expert Opin Ther Targets. 2012;16(1):67-83.

Stoss O, Werther M, Zielinski D, Middel P, Jost N, Rüschoff J, Henkel T, Albers P. Transcriptional profiling of transurethral resection samples provides insight into molecular mechanisms of hormone refractory prostate cancer. Prostate Cancer Prostatic Dis. 2008;11(2):166-72.

Sun X, Cheng G, Hao M, Zheng J, Zhou X, Zhang J, Taichman RS, Pienta KJ, Wang J. CXCL12 / CXCR4 / CXCR7 chemokine axis and cancer progression. Cancer Metastasis Rev. 2010;29(4):709-22.

Tamura K, Makino A, Hullin-Matsuda F, Kobayashi T, Furihata M, Chung S, Ashida S, Miki T, Fujioka T, Shuin T, Nakamura Y, Nakagawa H. Novel lipogenic enzyme ELOVL7 is involved in prostate cancer growth through saturated long-chain fatty acid metabolism. Cancer Res. 2009;69(20):8133-40.

Wang J, Shiozawa Y, Wang J, Wang Y, Jung Y, Pienta KJ, Mehra R, Loberg R, Taichman RS. The role of CXCR7/RDC1 as a chemokine receptor for CXCL12/SDF-1 in prostate cancer. J Biol Chem. 2008;283(7):4283-94.

Yun HJ, Ryu H, Choi YS, Song IC, Jo DY, Kim S, Lee HJ. C-X-C motif receptor 7 in gastrointestinal cancer. Oncol Lett. 2015;10(3):1227-1232.

Zhang B, Tian Y, Jin L, Li H, Shih IeM, Madhavan S, Clarke R, Hoffman EP, Xuan J, Hilakivi-Clarke L, Wang Y. DDN: a caBIG® analytical tool for differential network analysis. Bioinformatics. 2011 Apr 1;27(7):1036-8.

Zheng K, Li HY, Su XL, Wang XY, Tian T, Li F, Ren GS. Chemokine receptor CXCR7 regulates the invasion, angiogenesis and tumor growth of human hepatocellular carcinoma cells. J Exp Clin Cancer Res. 2010;29:31.

http://pharmaceuticalintelligence.com/2015/12/15/are-cxc4-antagonists-making-a-comeback-in-cancer-chemotherapy, 2015.

Supplementary File

DC3NET R SOFTWARE PACKAGE: Genome-wide differential gene network analysis software and an application in LnCap prostate cancer

Contents

1. Introduction

The *dc3net* is an R package that infers direct physical interactions of differential gene networks from gene expression datasets of multiple conditions. This supplementary file exemplifies how to use the *dc3net* package and express detailed information on the several workflows with example data sets. The data sets used in this file are available through the dc3net R-package. In the below figure, we present the DC3NET algorithm as block diagram:

Fig. 1. Schematic overview of the dc3net

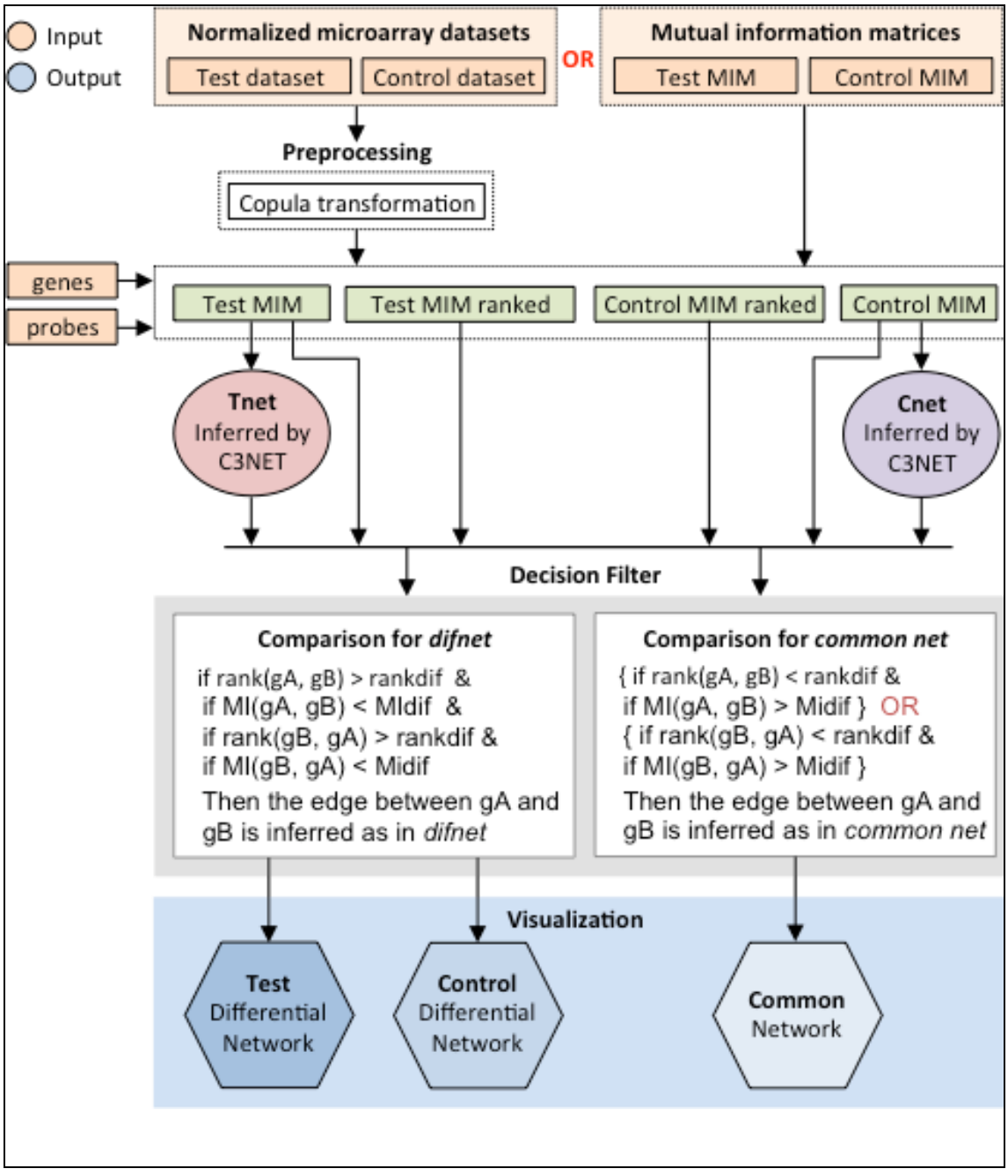

2. Installation of the R package DC3NET

Dc3net requires "R 3.2.x and later" and it depends on "*c3net*", "*igraph*" and "*RedeR*" packages that can be installed from the CRAN and Bioconductor libraries. For the installation of *dc3net*, the user needs to follow some simple installation steps.

1. To download and install dependent packages *c3net, igraph* and *RedeR* from CRAN and Bioconductor (execute in R):

```
> install.packages("c3net")
> install.packages("igraph")
> source("http://bioconductor.org/biocLite.R")
> biocLite("RedeR")
```

2. Execute the installation command for *dc3net* within R from CRAN or as follows:

```
> install.packages("https://github.com/altayg/dc3net/raw/master/dc3n
  et_1.2.0.tar.gz", type="source", repos=NULL)
```

3. For the instructions on the usage of *dc3net*, please check the user manual *dc3net-manual.pdf*

4. To load the library:

```
> library("dc3net")
```

3. General guidelines for using DC3NET

A detailed explanation and workflow of DC3NET algorithm can be found in (Altay et al., 2011). Therefore, we do not reproduce the open access text, but we briefly describe the DC3Net algorithm and explain the parameters we used on example data sets.

The required inputs of the package are two different gene expression data sets, probe names and gene names. Users can also use pre-computed test and control mutual information (adjacency) matrices as input. Otherwise, the algorithm takes the two data sets and generates the matrices itself. The data sets need to be normalized together (e.g. using RMA) before using in dc3net. If the input data sets are precomputed mutual information matrices, then the algorithm skip this preprocessing step. The MI matrices are square adjacency matrices where the MI value corresponds to the weight of interaction for each gene pair. The diagonals are set to zero to ignore self-interactions. The next step is computing row wise ranked versions of these MI matrices in descending order. Here, rank 1 corresponds to the highest mutual information value in a row of the matrix. This ranked matrices will be used in comparing and filtering the networks at the comparison step. Then C3NET is applied to the test and control MI matrices to infer gene networks of direct physical interactions of test and control datasets independently.

We integrated C3NET algorithm with DC3NET package, so we can use all functions of C3NET through DC3NET package's all in one command. All in one command of DC3NET is as follows:

```
> dc3net(data1, data2, probes, genes)
```

where the first two data set inputs are test and control data sets, e.g. tumor data and healthy data, respectively. Optional input parameters, *method*, *methodvalue*, *itnum*, *rankdif*, *percentdif*,

rankdcom, and *percentcom* are available to control the network inference and decision filtering steps. Furthermore, there are two more parameters, which are *probFiltered* and *visualization*. We recommend enabling *probFiltered* function, since it eliminates the interactions between the probes of the same gene. Visualization function plots the output networks. The visualization parameter takes three values, "0" for disabling the plot, "1" for plotting differential network and "2" for plotting common network. Users can adjust the parameters through command line. The example command above is the simple usage of DC3NET with default parameters.

The parameters that can be set are as follows:

```
method=cutoff

methodValue=0

itnum=1

rankDif=0

percentDif=0.6

rankdCom=0

percentCom=0.85

probFiltered=FALSE

visualization=0
```

The first three parameters, *method*, *methodvalue* and *itnum*, are belong to c3net package that are used to eliminate non-significant interactions (Altay and Emmert-Streib, 2010). The available options for *method* parameter are "cutoff", "justp", "rank", "holm", "hochberg", "hommel", "bonferroni", "BH" and "BY". *methodValue* and *itnum* parameters are dependent to *method* parameter. If the method is "cutoff", *methodValue* can be zero or predefined cut-off value. Zero means that mean of upper triangle will be taken as cutoff. If the method is "justp", *methodValue* and *itnum* (iteration number) parameters are need to be adjusted. For the "justp" method, *methodValue* corresponds to alpha value, e.g. 0.05. If the method is "rank", methodValue is the rank number. Rank corresponds to the number of interactions that will be taken as significant starting from the highest MI value. The other options, "holm", "hochberg", "hommel", "bonferroni", "BH" and "BY" are multiple testing correction (MTC) methods. Users can apply MTC methods easily by setting the name of MTC method to the method parameter. If the selected *method* is one of the MTC method, then *methodValue* and *itnum* parameters are need to be adjusted as it were in "justp" method. The default method was set to "cutoff" that uses mean of upper triangle of MI matrices as a significance threshold.

The next four parameters, *rankDif*, *percentDif*, *rankdCom* and *percentCom*, are for the comparison step of dc3net. This is the core part of DC3NET that we compare the two networks to find differential networks, *difnet* and *common network*. The order of `data1` and `data2` is important since the first data set is test network and the second one is control network. If we change the order of input data sets, we find *control difnet*, which consists of interactions that appears only in the control case. It is also crucial since it shows the required interactions of healthy cell.

In the comparison step of DC3NET, there are four conditions that all must be validated at the same time for an edge to be included in *test difnet*. Suppose that we check the potential interaction *geneA* to *geneB* to be included in *difnet* or not. As we stated above, we have been computed row wise ranked versions of the MI matrices in descending order. So we know the rank of interaction *geneA* to *geneB* in *control* MI matrix. The first parameter of DC3NET, *rankdif*, is the predefined cutoff parameter that checks the interaction between *geneA* and *geneB* is one of the top ranked interactions in control MI matrix or not. If the rank of *geneA* and *geneB* in the ranked *control* MI matrix is greater than the predefined cutoff parameter, *rankdif*, then the first condition becomes valid for deciding it as a difnet interaction. *rankdif* parameter can be adjusted to any value between 1 and number of rows of *control* MI matrix. However, if user wants a stricter *difnet*, then *rankdif* parameter needs to be adjusted to a greater value. The second condition is the change in MI value of interaction from *geneA* to *geneB* in the *control* MI matrix. Here, algorithm uses *MIdif* value as the cutoff parameter. *MIdif* is defined as *percentdif* times the maximum MI value of the row of *geneA* in the control MI matrix. Default value for the *percentdif* parameter is 0.6. Depends on strictness of the differential network, user can increase or decrease the second cutoff parameter. The previous two conditions compared the interaction of *geneA* to *geneB* but we also need to compare the interaction of *geneB* to *geneA*. So the algorithm validates the first and second conditions also for the interaction of *geneB* to *geneA*. In this example, if four of the conditions are validated, then DC3NET infer this interaction as in *test difnet* and continue to perform same filtering process for all gene pairs in *test network*.

Lets now start to describe the way that the algorithm infers the *common network*. *Common network* can be inferred by looking for all the same interactions between test and control network. However, this is a very strict way of inferring common network. So alternatively, one may consider the ranks and MI value decreases in the other data set. More broadly, users may follow the manner of the *difnet* process described above but change the comparison parameter, *rankdif*, from greater to less and for the *percentdif* from less to greater. Additionally, at this time, we only look at one of the two conditions, rather than all the four conditions together, from *geneA* to *geneB* or *geneB* to *geneA*. In the package, *rankdcom*, and *percentcom* parameters correspond to rank difference and MIdif for common network.

Finally, DC3NET infers *difnet* and *common network*, and assign them to the output environment. Furthermore, the package plots the selected inferred network according to the visualization parameter.

4. Data structure

4.1. Test data set

Load the example test data set contained in the *dc3net* package:

```
> data(tumorData)
```

The object `tumorData` is a tumor data matrix that contains gene expression data for the prostate cancer patients. The sample size is 52. This data was obtained from Broad Institute (Sing *et. al., 2002*). Since the size of the original data set is more than 1 GB, we added randomly selected 500 gene subset of the original prostate cancer data set to the package. This data set can be found in data folder of the package with the filename "tumorData.rda". The rows of the data set correspond to probes and the columns of the data set correspond to samples.

The dimension of the TEST data set:

```
> dim(tumorData)
[1] 500   52
```

4.2. Control data set

Load the example control data set contained in the *dc3net* package:

```
> data(normalData)
```

The object `normalData` is a normal data matrix that contains gene expression data for the prostate cancer patients. The sample size is 50. This data was also obtained from Broad Institute (Sing *et. al., 2002*). The data set can be found in data folder of the package with the filename "normalData.rda". The rows of the data set correspond to probes and the columns of the data set correspond to samples.

The dimension of the CONTROL data set:

```
> dim(normalData)
[1] 500   50
```

4.3. Probes

Load the gene annotation using one of the input data set. Assign gene annotation to probes parameter:

```
> probes <- rownames(tumorData)
```

4.4. Gene names

Load the example vector of gene names contained in the *dc3net* package:

```
> data(geneNames)
```

The object `geneNames` is an R vector that contains the names of the genes inside data sets above. The size of the vector should be equal to the number of rows in your data sets. You should input gene names that correspond to the probes in data sets otherwise the output networks would be produced with probe names. If you can't obtain the names of the genes, then you should run the *dc3net* command with putting gene annotation to third and fourth parameters e.g. Run dc3net without gene names:

```
> dc3net(tumorData, normalData, probes, geneNames)
```

5. LnCap example

Here, we show step by step, how to reproduce Figure 2 of the main paper. In this example, the default parameters were used.

```
> library(dc3net)
> data(LnCapTumorData)
> data(LnCapNormalData)
> data(geneNames)
> probes <- rownames(LnCapTumorData)
> networks <- dc3net(LnCapTumorData, LnCapNormalData, probes,
  geneNames, method="cutoff", methodValue=0, itNum=1, rankDif=2000,
  percentDif=0.3, rankdCom=100, percentCom=0.6, probFiltered=FALSE,
  visualization=TRUE)
```

This will compute differential and common networks with the parameters entered through command line. Both commands output differential network and common network tables that can be accessible by:

Differential Network Table:

```
> networks$DifNet
```

Common Network Table:

```
> networks$CommonNet
```

Users can also access to computed mutual information matrices of test and control data by using `networks$mimT` and `networks$mimC`. Thus, users can use this precomputed mutual information matrices on the next run of the algorithm to save time.

The example differential network can be seen in Table 1. In this table, first two columns show the names of the genes that their interactions are in differential or common network. The third column shows the mutual information values between genes. The interactions are sorted according to the mutual information values in descending order. So, the higher rank in the

table corresponds to higher interaction. The other columns of the tables can be helpful to advanced users. The fourth column, i, is the row number of the first gene and fifth column is the row number of max partner gene with highest MI value. Sixth and seventh columns are probes of the genes. The next columns are control index, MI rate of the first gene, rank of the first gene, MI rate of the second gene, rank of the second gene in control matrix, respectively.

DC3NET package is designed to inform users when operation continues. Some of the information are the parameters used, the cutoff value computed and dimensions of computed networks. One may easily tune parameters according to this information to obtain better results. The results of DC3NET can be validated through literature using R package, *ganet*. (Altay *et al.*, 2013).

Table 1. An example differential network output table of the *dc3net* (The first 10 rows)

Gene1	Gene2	MIval
LOC729384	SPRYD5	1.67144082
ABCC4	ACSL3	1.53963137
ORM1	TUBA3E	1.51528201
SLC41A1	STK39	1.51417854
TLL1	BCHE	1.47348983
GLUD1	SEPP1	1.47247699
ACSL3	IDH1	1.45508544
CENPN	ORM1	1.45459757
NCAPD3	CXCR7	1.42480939
C11orf92	UGT2B17	1.42160968

6. References

1. Altay G, Asim M, Markowetz F, Neal DE. Differential C3NET reveals disease networks of direct physical interactions. *BMC Bioinformatics*; 2011:12:296.
2. Altay G, Emmert-Streib F. Inferring the conservative causal core of gene regulatory networks. *BMC Systems Biology*; 2010:4:132.
3. Altay G, Altay N, Neal D. Global assessment of network inference algorithms based on available literature of gene/protein interactions. *Turkish Journal of Biology;* 2013:37:547-555.
4. Castro MAA. et al. RedeR: R/Bioconductor package for representing modular structures, nested networks and multiple levels of hierarchical associa-tions. *Genome Biology* 2012; 13(4):R29.
5. Singh D, Febbo PG, Ross K., et al. Gene expression correlates of clinical prostatecancer behavior. *Cancer cell*; 2002:1:203-9.